Proceedings of Science and Mathematics
Faculty of science, universiti teknologi malaysia

https://science.utm.my/procscimath/
Volume 27 (2024) 17-21

Antibacterial Activity of Phyto-Synthesized Silver Nanoparticles Using Different Organs of *Persicaria odorata*

Muhammad Hariz Asraf[a], Nik Ahmad Nizam Nik Malek[a,b]*, Nor Suriani Sani[c]**
[a]Department of Biosciences, Faculty of Science, Universiti Teknologi Malaysia, 81310 Skudai, Johor, Malaysia
[b]Centre for Sustainable Nanomaterials (CSNano), Ibnu Sina Institute for Scientific and industrial Research (ISI-SIR), Universiti Teknologi Malaysia, 81310 Skudai, Johor, Malaysia
[c]Department of Deputy Vice-Chancellor (Research and Innovation), Universiti Teknologi Malaysia, 81310 UTM Skudai, Johor, Malaysia
*Corresponding author: niknizam@utm.my
**Corresponding author: norsuriani@utm.my

Abstract
This study explores the antibacterial activity of silver nanoparticles (AgNPs) synthesized using *Persicaria odorata* leaf and stem extract. The optimized parameters included the volume of extract at 1 mL and 1 mM of $AgNO_3$ precursor concentration, having reaction times at 96 and 120 h, respectively. The AgNPs were characterized and tested against *Staphylococcus aureus* and *Escherichia coli*. Results revealed significant antibacterial efficacy, with notable inhibition zones for both AgNPs, with *S. aureus* showing higher susceptibility towards the AgNPs. These findings underscore the potential of *P. odorata*-mediated AgNPs as effective antibacterial agents, holding promise for addressing antibiotic resistance.
Keywords: Silver nanoparticles; *Persicaria odorata*; antibacterial

Introduction

The biosynthesis of silver nanoparticles (AgNPs) has emerged as a fascinating area of research due to its eco-friendly and sustainable approach. Unlike conventional chemical methods, biosynthesis utilizes biological entities such as plants, microbes, or fungi to reduce and stabilize silver ions, yielding nanoparticles with unique properties and applications [1]. This green synthesis method reduces environmental impact and offers advantages such as cost-effectiveness, scalability, and biocompatibility [2]. The resulting AgNPs will exhibit diverse functionalities, including antimicrobial, catalytic, and therapeutic properties, making them attractive for various industrial, medical, and environmental applications.

The biosynthesis of AgNP using *Persicaria odorata*, commonly known as Vietnamese coriander or daun kesum, has garnered considerable interest in recent years. This plant, renowned for its medicinal and aromatic properties, offers a sustainable and eco-friendly approach to nanoparticle synthesis. The bioactive compounds in *P. odorata* act as reducing and stabilizing agents during the green synthesis of AgNPs. This process eliminates the need for harmful chemicals and enhances the biocompatibility and therapeutic potential of the resulting nanoparticles [3].

Biosynthesized AgNP has demonstrated considerable potential in combating bacterial infections due to their distinctive properties. AgNP interacts with the cell membrane and penetrates the bacterial cell when applied to bacteria, initiating various antibacterial mechanisms [4]. Firstly, they disrupt the bacterial cell membrane, leading to structural damage and increased permeability, ultimately causing cell death through leakage of cellular contents. Secondly, AgNPs produce reactive oxygen species (ROS) within bacterial cells, such as superoxide radicals and hydrogen peroxide, inducing oxidative stress and cellular damage, contributing to bacterial cell death. AgNPs interfere with vital cellular processes in bacteria, including DNA replication, protein synthesis, and enzyme activity, disrupting essential functions and impeding bacterial growth and survival.

Furthermore, AgNPs can trigger apoptotic pathways in bacteria, leading to programmed cell death, thereby efficiently reducing bacterial populations [5]. Overall, utilizing biosynthesized AgNPs presents a promising strategy for addressing bacterial infections by targeting multiple cellular pathways and potentially synergizing with existing antibacterial agents. Ongoing research aims to optimize AgNP formulations and understand their precise mechanisms of action for enhanced efficacy and safety in clinical applications.

Different organs of *P. odorata* including its leaf and stem were extracted and used for the biosynthesis of AgNP to compare their effects on different parameters (volume of extract, concentration of $AgNO_3$, and reaction time) and antibacterial activity. In this work, the AgNPs were biosynthesized and optimized using different organs of *P. odorata* extract, and the AgNP was tested against pathogenic bacteria, namely *Escherichia coli* ATCC 11229 and *Staphylococcus aureus* ATCC 6538. The antibacterial activity of these two different organs used for the biosynthesis of AgNP was compared.

Materials and methods

P. odorata leaves were obtained from a local fresh market in Skudai, Johor, Malaysia, while silver nitrate powder was procured from WWR BDH Chemicals. The stems and leaves part of the *P. odorata* were separated. All media used for the antibacterial study, such as nutrient agar (NA) and Mueller-Hinton agar (MHA), were purchased from Oxoid. All bacterial strains were obtained from the glycerol stock culture, including *E. coli* ATCC 11229 and *S. aureus* ATCC 6538. Samples were abbreviated as leaf-synthesized AgNP (AgNP-L) and stem-synthesized AgNP (AgNP-S).

Fresh *P. odorata* were washed and rinsed. The leaves and stems were dried in an oven at 65°C overnight and ground separately to obtain a fine powder. The powder was stored at 4°C for later use. The synthesis of AgNP using different plant parts was conducted using the hot water extraction method. Thus, 1 g of the powder was mixed in the boiling water and stirred for 15 min. The extract was filtered through Whatman No. 1 filter paper and was kept at 4°C. Afterward, different volumes (0.2, 0.4, 0.6, 0.8, 1.0 mL) of the 1% leaf and stem extract were added to 10 mL $AgNO_3$ 1 mM solution. The mixtures were left for the reduction reaction to occur overnight at room temperature (27°C). The color change was recorded, and the visible spectrum (350 – 800 nm) was obtained using a visible spectrophotometer. Several parameters were recorded using the visible spectrophotometer to find the optimum condition of the AgNP colloidal formation, such as the volume of extract, concentration of $AgNO_3$, and reaction time. The parameters were carried out using one factor at the one-factor-at-a-time method.

The bacterial glycerol stock solution was thawed at room temperature (27°C). Then, a sterile inoculating loop was used to streak on a nutrient agar (NA) plate. The culture plates were then kept in an incubator at 37°C overnight to allow the growth and formation of single colonies. The cultured bacteria were sealed with a parafilm and kept in a 4°C fridge until further use. The bacteria were used based on the disc diffusion technique (DDT). The AgNP-L and AgNP-S colloidal solutions were adsorbed into cut filter paper disc at 100 µL and oven-dried. This step was repeated three times. The control samples were derived from ultrapure water (negative control) and kanamycin sulfate solution (positive control). A single colony was inoculated from the NA culture plates. Approximately 5 to 10 single colonies were inoculated using a sterile inoculating loop into a 5 mL saline solution. The samples' optical density (OD) was compared visually with 0.5 McFarland standard, a standard used as the turbidity adjustment equivalent to 1.5×10^8 CFU/ml of the bacterial suspension. The suspension was swabbed on the MHA agar surface while ensuring uniform growth. The discs were placed on the MHA agar surface using a sterilized tweezer, followed by a gentle press to ensure the pellet was attached firmly to the agar. The plate was inverted and incubated overnight at 37°C. The inhibition zones were measured (in cm) on the following day.

Results and discussion

The optimization parameters for the biosynthesis of AgNP using leaf and stem extract of *P. odorata* were carried out based on the different volumes of extract, different concentrations of $AgNO_3$ solution, and time required for the complete reduction of Ag ions (T_{max}). **Figure 1** shows the formation of a brownish colour of AgNP colloidal after reducing Ag ions into AgNP. AgNP-L indicated a higher intensity

of brown color compared to AgNP-S. The difference in the color intensity may indicate a different pattern of the AgNP spectrum based on the spectrophotometry.

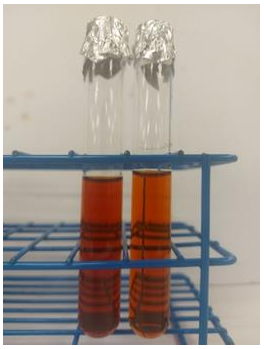

Figure 1 The color of colloidal AgNP when Ag ions were reduced for AgNP-L (left) and AgNP-S (right).

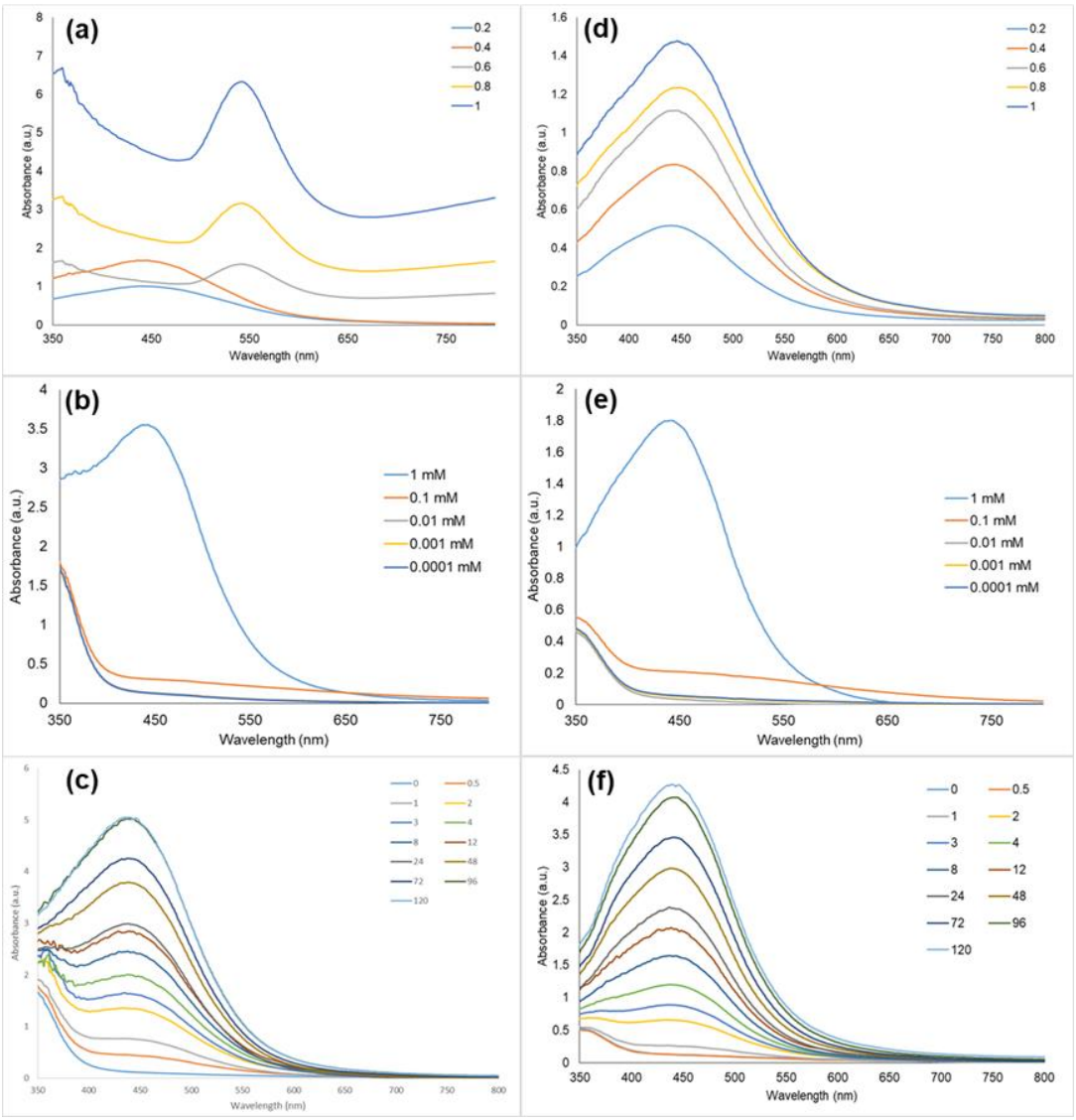

Figure 2 Vis-spectra of optimization parameters for AgNP-L (a, b, and c) and AgNP-S (d, e, and f). The parameters included volume of extract (a, d), AgNO3 concentration (b, e), and reaction time (c, f), respectively.

Figure 2 shows a higher intensity of surface plasmon resonance (SPR) peak of AgNP-L than that of AgNP-S. The intense peak is shown in **Figure 2(a, b, and c)** for AGNP-L. Although the SPR peak for AgNP-S is lower in intensity, both AgNP-L and AgNP-S showed prominent sharp peaks, indicating a good AgNP formation at 1 mL *P. odorata* extract. The first parameter indicated an increase in leaf extract volume would increase the SPR peak for both AgNP. However, AgNP-L showed a redshift of the peak as the volume of leaf extract increased from 0.4 to 0.6 mL, contributing to the formation of larger AgNP's size [6]. Also, the broad peaks formed at 0.2 and 0.4 mL signified a more agglomerated AgNP distribution [6]. On the other hand, the SPR of AgNP-S did not appear to shift at a different volume of stem extract.

The dilution of $AgNO_3$ concentration greatly affected the SPR formation for both AgNP. The ten-fold reduction from 1 mM of the $AgNO_3$ concentration significantly reduced the SPR peak of both AgNP. The absence of SPR peaks indicated no AgNP formation. The concentration of 0.1 mM $AgNO_3$ and lower was insufficient to react with the phytochemical compounds found in the extract chemically. Thus, the amount of synthesized AgNP was too small to be detected by the spectrophotometer.

The reaction time (T_{max}) of AGNP-L was faster than AgNP-S. AgNP-L took 96 h at max to complete the reduction reaction based on the optimized condition of 1% leaf extract, 1.0 mL extract volume, and 1 mM $AgNO_3$ concentration. Further observation at 120 h did not show any significant increase in the SPR peak. Otherwise, AgNP-L observed a slight increase in the SPR peak at 120 h. However, the increase started to become less significant denoting an almost complete reduction reaction.

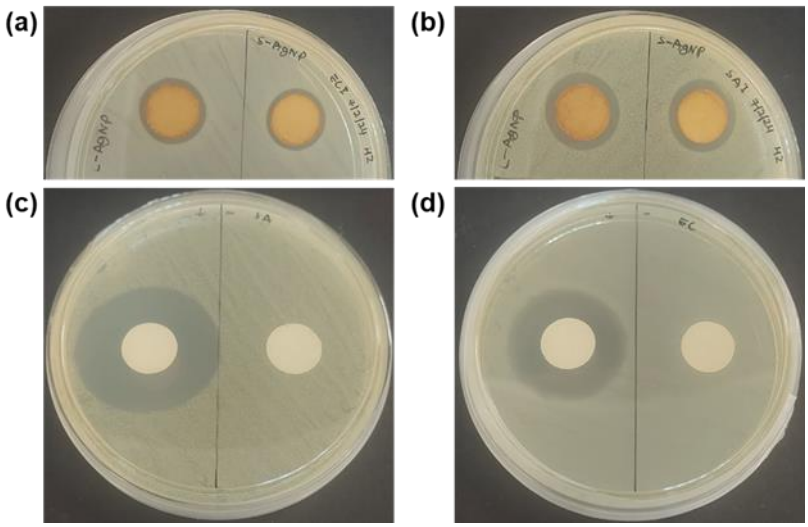

Figure 3 Inhibition zones formation of AgNP-L and AgNP-S against *E. coli* (a) and *S. aureus* (b). Control samples were also demonstrated to compare against both bacteria (c and d), respectively.

E. coli and *S. aureus* were proven to be susceptible to the AgNP-L and AgNP-S with similar antibacterial strength. Based on **Figure 3** and **Table 1**, AgNP-L and AgNP-S exhibit inhibition zones at 1.63 ± 0.06 cm against *E. coli* and 1.87 ± 0.06 cm against *S. aureus*. In comparison, *S. aureus* is more likely to be more susceptible than *E. coli.* The presence of an extra layer of peptidoglycan in gram-positive bacteria enables the adhesion or incorporation of the AgNP onto the membrane. Another study repurposed the AgNP by conjugating with other compounds, revealing that conjugated compounds with AgNP limited their permeability into the cytoplasm [7]. Instead, the conjugated AgNP caused disruption to the bacterial membrane and eventually killed the bacteria. The bacteria could not carry out their usual respiratory process, and the AgNP caused a blockage in the O_2 inter-membrane exchange. Besides that, AgNP also caused rupturing of the cell membrane when it directly came into contact. As reported previously, contact with AgNP caused membrane damage and deformation based on the microscopic observation of *S. aureus* [8].

Table 1: Inhibition zone (cm) of antibacterial assay for different colloidal samples.

Bacteria	Sample	Inhibition zone (cm)
E. coli	kanamycin sulphate	3.03 ± 0.06
	blank	0 ± 0
	AgNP-L	1.63 ± 0.06
	AgNP-S	1.63 ± 0.06
S. aureus	kanamycin sulphate	3.63 ± 0.06
	blank	0 ± 0
	AgNP-L	1.87 ± 0.06
	AgNP-S	1.87 ± 0.06

Conclusion

The production of AgNP using *P. odorata* extracts was found to be influenced by the extract volume, $AgNO_3$ concentration, and reaction time, with the leaf organ enhancing AgNP yield. Both AgNP-L and AgNP-S showed strong antibacterial activity against *E. coli* and *S. aureus*. This highlights the potential of *P. odorata* leaf extract as reducing and capping agent for AgNP that can be used as an antibacterial agent against a wide spectrum of bacteria.

Acknowledgement

The authors thank the Ministry of Higher Education Malaysia and Universiti Teknologi Malaysia for financial support (06E23 & 4J675). This work was also supported by the Malaysian Research University Network (MRUN) under the MRUN Research Officer Grant Scheme (MROGS) (Vo 5L004).

References

[1] P. Khandel, R.K. Yadaw, D.K. Soni, L. Kanwar, S.K. Shahi, Biogenesis of metal nanoparticles and their pharmacological applications: Present status and application prospects, *J. Nanostruct. Chem.* 8 (2018) 217–254. https://doi.org/0.1007/s40097-018-0267-4.

[2] S. Ahmed, M. Ahmad, B.L. Swami, S. Ikram, A review on plants extract mediated synthesis of silver nanoparticles for antimicrobial applications: A green expertise, *J. Adv. Res.* 7 (2016) 17–28. https://doi.org/10.1016/j.jare.2015.02.007.

[3] F.A. Lubis, N.A.N.N. Malek, N.S. Sani, K. Jemon, Biogenic synthesis of silver nanoparticles using Persicaria odorata leaf extract: Antibacterial, cytocompatibility, and in vitro wound healing evaluation, *Particuology*. 70 (2022) 10–19. https://doi.org/10.1016/j.partic.2022.01.001.

[4] A. Hamad, K.S. Khashan, A. Hadi, Silver nanoparticles and silver ions as potential antibacterial agents, *J. Inorg. Organomet. Polym. Mater.* 30 (2020) 4811–4828. https://doi.org/10.1007/s10904-020-01744-x.

[5] M.A. Radzig, V.A. Nadtochenko, O.A. Koksharova, J. Kiwi, V.A. Lipasova, I.A. Khmel, Antibacterial effects of silver nanoparticles on gram-negative bacteria: Influence on the growth and biofilms formation, mechanisms of action, *Colloids Surf. B Biointerfaces*. 102 (2013) 300–306. https://doi.org/10.1016/j.colsurfb.2012.07.039.

[6] A.A. Ashkarran, A. Bayat, Surface plasmon resonance of metal nanostructures as a complementary technique for microscopic size measurement, *Int. Nano Lett.* 3 (2013) 1–10. https://doi.org/10.1186/2228-5326-3-50.

[7] M.S. Zharkova, O.Y. Golubeva, D.S. Orlov, E. V. Vladimirova, A. V. Dmitriev, A. Tossi, O. V. Shamova, Silver Nanoparticles Functionalized With Antimicrobial Polypeptides: Benefits and Possible Pitfalls of a Novel Anti-infective Tool, *Front. Microbiol.* 12 (2021). https://doi.org/10.3389/fmicb.2021.750556.

[8] M.H. Asraf, N.A.N.N. Malek, N.S. Sani, J. Matmin, Surface morphology, porosity and antibiofilm activity of *Orthosiphon aristatus*-phytosynthesized–silver nanoparticles supported zeolite A, *Arab. J. Sci. Eng.* (2024). https://doi.org/10.1007/s13369-024-08832-x.